Mu opioid receptor knockout mouse: phenotypes with implications on restless legs syndrome

Shangru Lyu[1], **Mark P. DeAndrade**[1,*], **Erica L. Unger**[2], **Stefan Mueller**[3,*], **Alexander Oksche**[4,5], **Arthur S. Walters**[6], **Yuqing Li**[1]

[1.] Norman Fixel Institute for Neurological Diseases, Department of Neurology, College of Medicine, University of Florida, Gainesville, Florida, USA

[2.] Department of Biology, Lebanon Valley College, Annville, Pennsylvania, USA

[3.] Mundipharma Research GmbH & Co. KG, Höhenstraße 10, Limburg, Germany

[4.] Mundipharma Research Limited, Cambridge, UK

[5.] Rudolf-Buchheim-Institut für Pharmakologie, University of Giessen, Giessen, Germany

[6.] Division of Sleep Medicine, Vanderbilt University Medical Center, Nashville, Tennessee, USA

Abstract

Restless legs syndrome (RLS) is characterized by an irresistible need to move the legs while sitting or lying at night with insomnia as a frequent consequence. Human RLS has been associated with abnormalities in the endogenous opioid system, the dopaminergic system, the iron regulatory system, anemia, and inflammatory and auto-immune disorders. Our previous work indicates that mice lacking all three subtypes of opioid receptors have a phenotype similar to that of human RLS. To study the roles of each opioid receptor subtype in RLS, we first used mu opioid receptor knockout (MOR KO) mice based on our earlier studies using postmortem brain and cell culture. The KO mice showed decreased hemoglobin, hematocrit, and red blood cells (RBCs), with an appearance of microcytic RBCs indicating anemia. Together with decreased serum iron and transferrin, but increased ferritin levels, the anemia is similar to that seen with chronic inflammation in humans. A decreased serum iron level was also observed in the wildtype mice treated with an MOR antagonist. Iron was increased in the liver and spleen of the KO mice. Normal circadian variations in the dopaminergic and serotoninergic systems were absent in the KO mice. The KO mice showed hyperactivity and increased thermal sensitivity in wakefulness primarily during what would normally be the sleep phase similar to that seen in human RLS.

Corresponding author: Yuqing Li, Ph.D.; PO Box 100236, Gainesville, Florida 32610-0236; Phone 352-273-6546; Fax: 352-273-5989; yuqingli@ufl.edu.

Conflict of Interest Statement: none

Deficits in endogenous opioid system transmission could predispose to anemia of inflammation and loss of circadian variations in dopaminergic or serotonergic systems, thereby contributing to an RLS-like phenotype.

Introduction:

Restless legs syndrome (RLS) is a common heterogeneous sensorimotor disorder, which affects up to 10% of the population across the world (Garcia Borreguero, Winkelmann, & Allen, 2017). The prevalence of the disease is five times higher in iron-deficient people (Allen, Auerbach, Bahrain, Auerbach, & Earley, 2013; Allen & Earley, 2007; Connor, Patton, Oexle, & Allen, 2017; Trotti, 2017). RLS patients typically have a strong urge to move legs starting or worsening during the rest phase or inactivity, especially in the evening or at night, usually accompanied by abnormal sensations (Allen et al., 2014). There is at least partial and temporary relief of symptoms by movements (Trotti, 2017). Oral or intravenous iron can be used to improve symptoms in some RLS patients (Trotti & Becker, 2019). One of the primary treatments for RLS is dopaminergic agonists (Trotti, 2017). Oxycodone, an agonist for opioid receptors, in combination with naloxone, an antagonist for opioid receptors added to relieve constipation, has been approved in Europe as second-line therapy for refractory RLS (Trenkwalder et al., 2013).

Previous studies have shown that RLS patients exhibit an endogenous opioid deficiency of beta-endorphin and met-enkephalin in the thalamus (A. S. Walters, Ondo, Zhu, & Le, 2009). A brain imaging study demonstrates significant negative correlations between opioid receptor binding potential in brain regions involved in the medial affective pain system and the severity of RLS symptoms (von Spiczak et al., 2005). Our *in vitro* work showed that cultured dopaminergic neurons treated with deferoxamine, an iron-chelating agent, show decreased cell survival (Sun, Hoang, Neubauer, & Walters, 2011). The damage is mostly prevented by the application of endogenous opioid analog before iron chelation (Sun et al., 2011), suggesting interactions among the opioid system, iron deficiency, and dopaminergic dysfunction. Our recent *in vivo* work showed that mice with genetic disruption of all three subtypes of opioid receptor (MOR, DOR, KOR) genes (triple KO) exhibit hyperactivity and a trend of increased probability of waking during the rest period (day) akin to that in human RLS (night) (Lyu, DeAndrade, et al., 2019). Surprisingly, triple KO mice also show decreased serum iron concentration, evidence of anemia, altered dopamine metabolism, as well as decreased thermal sensation (Lyu, DeAndrade, et al., 2019) similar to that seen in human RLS. However, it is not known which subtype of opioid receptors is directly responsible for the RLS-like phenotypes in the triple KO mice.

The current investigation extended our previous work to allow allocation to a specific receptor subtype, mu opioid receptor (MOR). We started from the MOR instead of DOR and

KOR because our earlier work on postmortem human RLS brains shows a deficiency of beta-endorphin and met-enkephalin in the thalamus (A. S. Walters et al., 2009), suggesting the involvement of MOR in RLS. With MOR knockout (KO) mice, we analyzed both behavioral and biochemical abnormalities relevant to the human RLS. Instead of aiming for developing an RLS animal model for preclinical drug testing and model the disease, the study is to test the role of the endogenous opioid system in the iron homeostasis, the development of anemia, and circadian rhythm changes in the dopaminergic and serotonergic systems. We hypothesized that genetic disruption of only MOR gene would cause dysregulated iron homeostasis and monoamine systems.

Material and methods:

Animals

The MOR KO mice (*Oprm1^{tm1Kff}*) were from Jackson Laboratory (Stock No: 007559, RRID: IMSR_JAX:007559). The original MOR KO mice were bred with the wild-type (WT) mice to generate heterozygous males and females, which were interbred to generate experimental animals. Pups were weaned about 21 days after birth and housed as 5 pups per cage within a specific-pathogen-free (SPF) facility in standard mouse cages at 21°C under normal 12-hr light, 12-hr dark (12 LD) cycle condition. The light was on at 6:00 am and off at 6:00 pm. The colony had a quarterly monitoring program of common rodent pathogens conducted by the Animal Care Service of the University of Florida. All experimental animals (97 male MOR KOs, 4 female MOR KOs, 77 male WTs, 5 female WTs) were littermates except for the experiment with naloxonazine, in which 21 WT mice were used. The generation and maintenance of animals varied due to natural survival. The mean age of animals was 163 days, with a 95% confidence interval from 149 to 176 days. Most of the experiments were conducted with males to minimize the variations caused by estrous cycles in females. The tissue iron measurement was conducted in both males and females. All animal experiments that comply with the ARRIVE guidelines were carried out in accordance with the National Institutes of Health guide for the care and use of laboratory animals (NIH Publications No. 8023, revised 1978). When euthanized by asphyxiation of CO_2, mice were placed in the animal cage with euthanasia lid on and 1.3 LPM CO_2 for at least 3 min plus 10 LPM CO_2 for at least 1 min, followed by cervical dislocation. Investigators who conducted the experiments were unaware of the genotypes of the animals studied.

Colorimetric assay for serum iron, ferritin, and transferrin

Blood was collected by cardiac puncture method from nine MOR KO and four WT male mice with an average age of six months. The blood was allowed to clot and then separated by centrifugation at 1,500 g for 10 min. The serum was removed and centrifuged again at 1,500 g for 10 min for further purification. The serum transferrin levels were determined using the Mouse Transferrin ELISA Kit (Immunology Consultants Laboratory Inc.). Only six KO samples were available for iron and ferritin quantification, which were measured by QuantiChrom Iron Assay Kit (BioAssay Systems Inc.) and Mouse Ferritin ELISA Kit (Immunology Consultants Laboratory Inc.), respectively.

Quantification of tissue iron

Spleen, liver, and striatum were dissected from ten MOR KO (seven males, four females) and ten WT (five males, five females) mice with an average age of four months and immediately frozen in liquid nitrogen. The tissue samples were stored at −80 °C until use. The experiment was done as described previously (DeAndrade et al., 2012). Striata and spleens were thawed on ice and homogenized in phosphate buffered saline (PBS, 9.1 mM Na_2HPO_4, 1.7 mM NaH_2PO_4, 150 mM NaCl, pH 7.4) containing protease inhibitors (10mL/g tissue; Roche, Indianapolis IN). For iron analysis, ultra-purified nitric acid was added to a total of 10 ul of each homogenate in a polypropylene microfuge tube. Samples were digested for 48 hrs at 50ºC and then diluted 1:10 for striata and 1:500 for spleens with 3.12 mmol/L nitric acid. Prepared samples were analyzed in duplicate using a graphite furnace atomic absorption spectrometer (PerkinElmer AAnalyst 600, Shelton, CT). Standards were prepared by diluting a Perkin Elmer iron standard (PE#N9300126) in 0.2% ultra-purified nitric acid, and blanks were prepared with digesting and diluting reagents to control for possible contamination. Only six male samples were available for measuring levels of the liver iron, which were determined by colorimetric assay using the procedure described before (Torrance & Bothwell, 1968), with ferrozine as the color reagent. Absorbances of duplicate samples were measured at a wavelength of 535 nm. The standard curves for all iron measurements exceeded $r > 0.99$.

Mineral measurement in striatal tissues

Thirteen MOR KO males and eleven WT males with an average age of four months were sacrificed and perfused with ice-cold saline. Their striata were dissected out and quickly frozen with liquid nitrogen. The samples were shipped to the Veterinary Diagnostic Laboratory of Michigan State University and measured by atomic absorption spectroscopy.

In vivo pharmacology

Naloxonazine (Sigma-Aldrich, CAS No. 880759-65-9) (an irreversibly binding MOR antagonist) was injected into twelve WT male mice intraperitoneally at 20 mg/kg. The other nine WT male mice received saline injection as control. The average for the mice was three months. After seven consecutive days of injections, mice were sacrificed on the eighth day, and their serums were collected. Serum iron, ferritin, and transferrin were measured as described above.

Complete blood count (CBC)

Blood was collected by cardiac puncture from eleven MOR KO and four WT male mice with an average age of five months. The blood was analyzed with a HemaVet machine (The Americas Drew Scientific Inc.) by the ACS Clinical Diagnostics Laboratory of the University of Florida.

Striatal monoamine analysis

Nine MOR KO and eight WT male mice, and another cohort of twelve MOR KO and ten WT male mice, with an average age of seven months, were sacrificed during the midday and the midnight, respectively. Their striata were dissected out and quickly frozen with liquid

nitrogen. The samples were analyzed by the Neurochemical Core of Vanderbilt University to obtain dopamine (DA) and serotonin (5-HT) as well as their respective metabolites 3,4-dihydroxyphenylacetic acid (DOPAC), homovanillic acid (HVA) and 5-hydroxyindoleacetic acid (5-HIAA) (DeAndrade et al., 2012).

Western blot

Antibodies used and their concentrations.

Name	Structure of the immunogen	RRID	Concentration
D1DR Antibody	D1DR (G-18)	Santa Cruz Biotechnology, Cat# sc-31478, RRID: AB_2261889, goat, polyclonal	1:200
D2DR Antibody	D2DR (B-10)	Santa Cruz Biotechnology, Cat# sc-5303, RRID: AB_668816, mouse, monoclonal	1: 1000
DAT Antibody	DAT (C-20)	Santa Cruz Biotechnology Cat# sc-1433, RRID: AB_631362, goat, polyclonal	1: 1000
GAPDH Antibody	GAPDH (V-18)	Santa Cruz Biotechnology, Cat# sc-20357, RRID: AB_641107, goat, polyclonal	1:2000
IRDye® 680RD Donkey anti-Goat IgG Secondary Antibody	Goat IgG	LI-COR Biosciences, Cat# 926-68074, RRID: AB_10956736, donkey	1:15,556
IRDye® 800CW Donkey anti-Mouse IgG Secondary Antibody	Mouse IgG	LI-COR Biosciences, Cat# 926-32212, RRID: AB_621847, donkey	1:15,556
IRDye® 800CW Donkey anti-Goat IgG Secondary Antibody	Goat IgG, whole molecule	LI-COR Biosciences, Cat# 926-32214, RRID: AB_621846, donkey	1:15,556

Western blot was performed as previously described (Yokoi et al., 2015). The striata were dissected from six MOR KO and six WT male mice with an average age of two months and homogenized in 200 μl of ice-cold lysis buffer (Tris/HCL 50mM, pH=7.4; NaCl 175mM; EDTA 5mM, pH=8.0) containing protease inhibitor cocktail (Roche). 22 μl of ice-cold 10% Triton X100 was added in the homogenate. The mixtures were incubated for 30 min on ice and centrifuged at $10,000 \times g$ for 15 min at 4°C. The supernatant was used as protein samples for western blots. The protein concentration of the supernatant was measured by protein assay reagent (Bio-Rad). An aliquot of the supernatant was mixed with loading buffer containing 2-mercaptoethanol and boiled for 5 min, chilled on ice and spun down. The proteins were separated on a 10% SDS-PAGE gel and transferred to Millipore Immobilon –FL transfer membranes (PVDF). The PVDF membranes were washed in 0.1M PBS for 5 min and blocked with LI-COR Odyssey blocking buffer for 1 hr. The membranes were incubated overnight at 4°C with goat polyclonal D_1R antibody (Santa Cruz Biotechnology Cat# sc-31478, RRID: AB_2261889) at 1:200 dilution, mouse monoclonal D_2R antibody (Santa Cruz Biotechnology Cat# sc-5303, RRID: AB_668816) at 1:1000 dilution, goat polyclonal dopamine transporter (DAT) antibody (Santa Cruz Biotechnology Cat# sc-1433, RRID:AB_631362) at 1:1000 dilution, or goat glyceraldehyde-3-phosphate dehydrogenase (GAPDH) antibody (Santa Cruz Biotechnology Cat# sc-20357, RRID: AB_641107) at 1:2000 dilution in the blocking buffer. The membranes were washed with 0.1M PBS containing 0.1% Tween 20 for 4 times of 5 min each, then treated for 1 hour with

LI-COR IRDye 680RD donkey anti-goat IgG (H+L) (LI-COR Biosciences Cat# 926-68074, RRID: AB_10956736), LI-COR IRDye 800CW donkey anti-mouse IgG (H+L) (LI-COR Biosciences Cat# 926-32212, RRID: AB_621847), or LI-COR IRDye 800CW donkey anti-goat IgG (H+L) (LI-COR Biosciences Cat# 926-32214, RRID: AB_621846) at 1:15,556 dilution. After washing four times of 5 min each with 0.1M PBS containing 0.1% Tween 20 and 0.1M PBS 3 times for 5 min each, the membranes were dried, and the signals were detected and quantified by an LI-COR Odyssey imaging system.

Behavioral studies

Five MOR KO and five wild type (WT) adult male mice with an average age of twelve months were used in the wheel running analysis as previously described (DeAndrade et al., 2012). Briefly, each mouse was placed in a wheel running chamber with enough corncob bedding, nestlets, food and water under the 12 LD condition. Wheel running activity was recorded as the number of wheel revolutions occurring during 5 min bins using Lafayette Instrument Activity Wheel Monitor software. The activity from the last two days was included in the data analysis, grouped by light and dark phases.

Fourteen MOR KO and fourteen WT male mice with an average age of four months were tested for the perception of warm stimuli (Lyu, Xing, DeAndrade, Perez, et al., 2019). Each mouse was placed in an acrylic restrainer with the distal end of its tail protruding on a metal surface maintained at 55°C during the day or rest period. The timer was turned on once the tail touched the surface and immediately stopped when the mouse flicked its tail away from the heat.

The second cohort of six MOR KO and five WT male mice with an average age of ten months were tested for the circadian variation of the thermal sensation and the effect of dopaminergic treatment. The tail-flick experiment was conducted during the middle of the active phase (approximately 0:00 AM), the middle of the rest phase (approximately 12:00 PM), and 30 min following an intraperitoneal injection of ropinirole at 0.1 mg/kg of body weight (approximately 3:00 PM). Ropinirole is a common dopaminergic treatment of RLS.

Food and water intake

The experiment was conducted essentially according to others (Bachmanov, Reed, Beauchamp, & Tordoff, 2002). Five MOR KO and five WT male mice with an average age of eight months were acclimated to individual cages for 6 days. Food and water intakes were measured daily for 4 days. During the test, deionized water was available from a 25 ml plastic serological pipette with 0.2 ml gradations inserted into the cage. The top of the pipette was closed with a rubber stopper. The drinking tubes were placed to the mouse's right of the food hopper. The sprouts were 25 mm above the cage bottom. Water intake was calculated from the scale on the pipette and food intake was derived from the weight of the whole cage. The body weights of the mice were measured at the beginning and the end of the 4-day test period.

Data processing and statistical analysis

Peripheral iron and Western blot results were compared with the Student's t-test. Other data were first tested for normality using an SPSS version 25 statistical package. Tissue iron, ferritin and transferrin levels in the serum after the drug injection, striatal mineral measurements, most of the blood profiles, HPLC data and food-water consumption of the WT and the MOR KO were normally distributed and therefore compared by mixed model ANOVA (SAS 9.1 statistical package). The results from Student's t-test and mixed model ANOVA were presented as mean ± standard deviation (SD) in the text. Serum iron after the drug injection, platelet count and tail-flick data were not normally distributed and analyzed by the generalized linear mixed model (GENMOD) with a gamma distribution. Wheel running data was analyzed by GENMOD with a negative binomial distribution. Observations of microcytic or hypochromic anemia were analyzed by Fisher's exact test. The p values in the HPLC data have been adjusted for multiple comparisons using the Benjamini-Hochberg-Yekutieli false discovery rate [FDR ($p < 0.05$)].

To generate hourly activities as presented in Figures 5A and B, we processed the data as described before (Lyu, Xing, DeAndrade, Liu, et al., 2019). The interval counts collected every 5 min during each hour were summed for each animal. Wheel running activity during the last 48 hrs was analyzed. Each animal had 12 data points for each hour in the wheel running test. The average interval counts within each hour were calculated for each genotype. The significant p values, calculated by GENMOD with a negative binomial distribution grouped by each hour, were marked above the corresponding times in the figures.

Age was considered as a variable in the statistical model for the data in Figures 4 (Table 3) and 6 (Table 5). This is because, within each experimental cohorts, individual animals differed in age and were not born on the same date. For Figure 4 (Table 3), animals sampled during midday were 213 ± 64 (mean ± standard deviation) days old, and animals tested at midnight were 214 ± 17 days of age. For Figure 6 (Table 5), the first cohort was 120 ± 37 days of age, and the second cohort was 303 ± 236 days of age. A mixed model or the GENMOD can adjust the age difference.

Results:

Altered iron metabolism, blood profile and striatal mineral concentrations in the MOR KO mice

Lower peripheral iron level is thought to be correlated with the development of RLS, and the occurrence of RLS is higher in people with the iron deficiency than in the general population (Connor et al., 2017). Ferritin is predominantly a cytosolic iron storage protein and helps to protect cells from potentially toxic effects such as hydroxyl radical formation. Transferrin binds to iron and helps iron transportation to cells, which take up transferrin via transferrin receptors 1 and 2 (Tfr1, Tfr2). Both ferritin and transferrin are important proteins involved in iron homeostasis (Anderson & Frazer, 2017). Ferritin is also considered as an inflammatory biomarker, which is increased in several disease states such as NFALD, type 2 diabetes mellitus and metabolic syndrome (Kell & Pretorius, 2014). Therefore, we first measured the

concentrations of iron, ferritin, and transferrin in the serum. We found that iron and transferrin levels were decreased, while the ferritin level was increased in the MOR KO mice (Figure 1A, WT, 212.85 ± 28.72, n=4; KO, 167.45 ± 31.76, n=6; t_8=2.29, p=0.05; B, WT, 2695.49 ± 816.53, n=4; KO, 3947.81 ± 583.20, n=6; t_7=2.69, p=0.03; C, WT, 590.60 ± 64.01, n=4; KO, 344.08 ± 172.70, n=9; t_{11}=3.74, p<0.01; all unpaired Student's t-test). Further, in a CBC test, we found significantly decreased levels of red blood cells (RBCs), hemoglobin (HB) and hematocrit (HCT) (Table 1, RBC: WT, 9.91 ± 1.12, n=4; KO, 8.01 ± 1.03, n=11; $F_{1,12}$=5.74, p=0.03; HB: WT, 12.26 ± 1.09, n=4; KO, 9.77 ± 1.52, n=11; $F_{1,12}$=5.42, p=0.04; HCT: WT, 40.21 ± 4.23, n=4; KO, 32.26 ± 4.69, n=10; $F_{1,11}$=5.18, p=0.04; all mixed model ANOVA) in the MOR KO mice. HB is a protein in RBCs that carries oxygen throughout the body. HCT measures the percentage of RBCs in the blood. A reduced number of RBCs, as well as low values of HB and HCT, indicate a state of anemia. Also, we observed a trend of more microcytic and hypochromic RBCs in mutant mice, which was absent in the WTs (Table 1, microcytic or hypochromic RBC: WT, n=4, KO, n=11, p=0.10, Fisher's exact test). The results suggest that MOR KO mice show signs of anemia of inflammation (AI) with low serum iron, decreased transferrin levels and increased ferritin levels. We also measured iron levels in tissues, including striatum, spleen, and liver (Table 2). Both males and females were used in the experiment so that we first tested the interaction between sex and genotype (sex X genotype) in each case. We found that the iron level in spleen had no sex and genotype interaction ($F_{1,17}$=0.01, p=0.91; Figure 2B, WT, 739.20 ± 467.63, n=10; KO, 1118.70 ± 336.62, n=11; $F_{1,18}$=4.38, p=0.05; sex, $F_{1,18}$=1.00, p=0.33; all mixed model ANOVA) and were elevated. For the liver, sex and genotype did not interact (sex X genotype, $F_{1,16}$=0.89, p=0.36, mixed model ANOVA) and sex was significant ($F_{1,17}$=9.92, p<0.01) when the interaction was removed. Therefore, we analyzed the iron level in the liver as post hoc, with the two sexes separated. Increased iron level was found in the male liver (Figure 2C, male, WT, 98.16 ± 45.37, n=5; KO, 154.34 ± 58.89, n=6; $F_{1,9}$=3.03, p=0.05, mixed model ANOVA). WT female mice had higher iron levels than WT male mice but showed no difference vs MOR KO female mice (Figure 2C, female, WT, 178.75 ± 34.46, n=5; KO, 197.46 ± 12.66, n=4; $F_{1,7}$=1.04, p=0.53, mixed model ANOVA). The liver is the site for iron storage while the spleen is the site for iron recycling (Anderson & Frazer, 2017). Increased hepatic and splenic iron implies a dysfunction in iron storage and recycling. In AI patients, iron is sometimes elevated in the body tissues (Wessling-Resnick, 2010). In this sense, the findings of elevated iron in the liver and spleen are compatible with AI. Despite the marked decrease in serum iron and transferrin levels, we did not find striatal iron changes (sex X genotype, $F_{1,17}$=0.59, p=0.45; Figure 2A, WT, 23.87 ± 4.70, n=10; KO, 23.16 ± 6.46, n=11; $F_{1,18}$=0.10, p=0.76; sex, $F_{1,18}$=5.10, p=0.04; all mixed model ANOVA; Supplementary Table 1, WT, 78.27 ± 16.36, n=11; KO, 115.10 ± 122.93, n=13; $F_{1,20}$=0.91, p=0.35, mixed model ANOVA). When analyzed the data separately by sex since it reached significance after the interaction was removed, the striatal iron levels were still the same between the two groups (Male: WT, 22.18 ± 4.00, n=5; KO, 19.92 ± 4.95, n=7; $F_{1,18}$=0.70, p=0.42; Female: WT, 25.57 ± 5.15, n=5; KO, 26.88 ± 6.99, n=4; $F_{1,18}$=0.11, p=0.75; all mixed model ANOVA). However, significant increases of other minerals, like copper, molybdenum, selenium, and zinc were observed in the striata of MOR KO male mice (Supplementary Table 1, copper: WT, 17.54 ± 1.60, n=11; KO, 19.18 ± 1.74, n=13; $F_{1,20}$=5.53, p=0.03; molybdenum: WT, 0.18 ± 0.03, n=11; KO, 0.21 ± 0.03, n=13;

$F_{1,20}$=5.45, p=0.03; selenium: WT, 1.13 ± 0.09, n=11; KO, 1.23 ± 0.10, n=13; $F_{1,20}$=8.46, p<0.01; zinc: WT, 69.99 ± 6.80, n=11; KO, 76.84 ± 7.70, n=13; $F_{1,20}$=8.82, p<0.01; all mixed model ANOVA). Increased incorporation of zinc into protoporphyrin IX and heme in RBCs has been reported in 19 patients with AI, which is probably caused by an impairment of iron metabolism (Hastka, Lasserre, Schwarzbeck, Strauch, & Hehlmann, 1993). The higher level of zinc found in the MOR KO striatum is therefore consistent with a state of AI and dysfunction in iron hemostasis. These results are also consistent with our previous report of increased levels of zinc in both serum and brain of RLS patients as measured by laser capture (A.S. Walters et al., 2016). The effectiveness of selenium in the treatment of RLS has been reported (Rahimdel, Ayatollahi, Zeinali, Mehrabanian, & Mellat-Ardekani, 2012; Ulfberg, Stehlik, & Mitchell, 2016). The increased selenium found in the MOR KO mice may be a compensatory result.

Overall, results of CBC, changes in iron, ferritin, and transferrin levels and altered tissue minerals favor AI more than iron deficiency anemia in MOR KO mice (Weiss & Goodnough, 2005). Although both types of anemia may have low serum iron and microcytic/hypochromic RBCs, which is what we showed in the KO mice, the serum ferritin is usually increased in AI as in the present case vs being decreased as it usually is in iron deficiency anemia. In addition, serum transferrin is increased in iron deficiency anemia and decreased in AI, so the decreased transferrin in our experiments goes in favor of AI and not iron deficiency anemia. Tissue iron is decreased in iron deficiency anemia and increased in AI, so the increased iron in liver and spleen in our experiments further supports AI vs iron deficiency anemia. These findings are in line with published literature according to which 95% of the highly-associated RLS conditions, defined as conditions under which RLS have shown to have a statistically higher prevalence, like multiple sclerosis and rheumatoid arthritis, are associated with inflammatory or immune alterations (Weinstock, Walters, & Paueksakon, 2012). Therefore, our data imply a relationship among MOR, inflammation, and RLS.

Injection of a MOR antagonist decreased the iron level in mouse serum

To analyze whether a decrease in serum iron could also be elicited by pharmacological blockade of MORs, we injected the irreversibly binding MOR antagonist naloxonazine intraperitoneally into the WT mice for 7 days. Only male mice were used to minimize the estrous cycle variation and to be consistent with the experiment in which MORs were genetically knocked out (Figure 1). The data were analyzed by SAS GENMOD, which gives out an estimate (ES), standard error (SE), and 95% confidence interval (95%CI) for MOR KO relative to WT. The latter was normalized to 0. We found that naloxonazine decreased the serum iron level (Figure 3A, saline, 154.46 ± 81.67, n=9; naloxonazine, 121.19 ± 38.01, n=12, ES, −0.18, SE, 0.09, 95%CI, −0.36 and 0.00; Z=3.05, p=0.05, GENMOD with gamma distribution) but did not cause significant alterations in ferritin and transferrin levels (Figure 3B, saline, 2126.71 ± 688.40; n=9, naloxonazine, 2585.79 ± 931.08, n=12; $F_{1,18}$=3.65, p=0.07; 3C, saline, 4031.06 ± 2486.88, n=9; naloxonazine, 4111.80 ± 1938.30, n=12; $F_{1,18}$=0.02, p=0.88; all mixed model ANOVA). Our data indicate that short-term pharmacological modulation (7 days) of MOR in male mice is sufficient to cause peripheral iron deficiency albeit transferrin and ferritin remained unchanged.

Lack of circadian variations of the dopaminergic and serotonergic system in the MOR KO mice

One of the most common treatments for RLS is levodopa and dopamine D_2/D_3 receptor (D_2/D_3R) agonists (Wanner, Garcia Malo, Romero, Cano-Pumarega, & Garcia-Borreguero, 2019). Clinical studies have revealed significant alterations in the dopaminergic systems of RLS patients (Christopher J. Earley, Uhl, Clemens, & Ferré, 2017). We compared the striatal protein levels of dopamine receptors (D_1R, D_2R) and dopamine transporters (DAT) between the MOR KO and their WT littermates. We did not find any changes in the protein expression levels with male mice (Supplementary Figure 1, D_1R: WT, 0.36 ± 0.08, n=6; KO, 0.35 ± 0.06, n=6; t_9=0.30, p=0.77; D_2R: WT, 0.12 ± 0.04, n=6; KO, 0.13 ± 0.03, n=6; t_{10}=0.26, p=0.80; DAT: WT, 0.69 ± 0.22, n=6; KO, 0.51 ± 0.11, n=6; t_7=1.78, p=0.11; all unpaired Student's t-test).

HPLC analysis was performed with mice sacrificed during the midday and midnight (named as "Time" in the data analysis) to determine striatal levels of DA, 5-HT and their metabolites. The interactions among age, genotype and time were assessed first and no significance were observed (NA, $F_{1,34}$=0.11, p=0.74; DOPAC, $F_{1,34}$=0.01, p=0.94; DA, $F_{1,34}$=0.17, p=0.68; 5-HIAA, $F_{1,34}$=0.02, p=0.88; HVA, $F_{1,34}$=0.09, p=0.77; 5-HT, $F_{1,34}$=1.50, p=0.23; 3-MT, $F_{1,34}$=0.00, p=0.96; DOPAC/DA, $F_{1,34}$=1.48, p=0.23; HVA/DA, $F_{1,34}$=0.19, p=0.66; 5-HIAA/5-HT, $F_{1,34}$=0.32, p=0.58; 3-MT/DA, $F_{1,34}$=0.38, p=0.54; all mixed model ANOVA). Then, the interactions between genotype and time were calculated. Significant interactions were found between genotype and time only in DA, HVA, 5-HIAA/5-HT and 3-MT/DA (NA, $F_{1,34}$=0.46, p=0.50; DOPAC, $F_{1,34}$=3.45, p=0.07; DA, $F_{1,34}$=6.72, p=0.01; 5-HIAA, $F_{1,34}$=2.63, p=0.11; HVA, $F_{1,34}$=5.86, p=0.02; 5-HT, $F_{1,34}$=0.00, p=0.98; 3-MT, $F_{1,34}$=0.81, p=0.37; DOPAC/DA, $F_{1,34}$=1.22, p=0.28; HVA/DA, $F_{1,34}$=0.01, p=0.94; 5-HIAA/5-HT, $F_{1,34}$=4.51, p=0.04; 3-MT/DA, $F_{1,34}$=1.72, p=0.20; all mixed model ANOVA). Therefore, the data were analyzed separately based on either genotype or time. There were no significant changes in levels of all neurotransmitters tested in the male MOR KO mice compared with their male WT littermates both during the day (Supplementary Table 2) and during the night (Supplementary Table 3). However, when comparing the levels of these monoamines between the day and the night in each genotype (Table 3), we found that WT mice had lower midday (rest phase for mice) levels compared to midnight (active phase for mice) levels for DA (Figure 4A, WT, midday, 127.18 ± 33.45, n=8; midnight, 199.01 ± 22.78, n=10; $F_{1,15}$=29.43, p<0.01; age, $F_{1,15}$=1.52, p=0.43, mixed model ANOVA), DOPAC (Figure 4B, WT, midday, 8.58 ± 2.47, n=8; midnight, 11.46 ± 1.53, n=10; $F_{1,15}$=12.37, p<0.01; age, $F_{1,15}$=7.26, p=0.10, mixed model ANOVA), and HVA (Figure 4C, WT, midday, 14.76 ± 3.21, n=8; midnight, 18.94 ± 3.04, n=10; $F_{1,15}$=8.46, p=0.02; age, $F_{1,15}$=2.42, p=0.39, mixed model ANOVA). The turnovers of DA and serotonin, on the other hand, were lower during the night (Figure 4D, WT, midday, 0.07 ± 0.01, n=8; midnight, 0.06 ± 0.01, n=10; $F_{1,15}$=16.11, p<0.01; age, $F_{1,15}$=13.17, p=0.03; E, WT, midday, 0.07 ± 0.01, n=8; midnight, 0.06 ± 0.01, n=10; $F_{1,15}$=9.87, p=0.01; age, $F_{1,15}$=0.65, p=0.59; F, WT, midday, 0.20 ± 0.03, n=8; midnight, 0.26 ± 0.04, n=10; $F_{1,15}$=12.15, p<0.01; age, $F_{1,15}$=0.85, p=0.58; all mixed model ANOVA). Surprisingly, these circadian variations in dopaminergic and serotonergic systems found in WTs were absent in the male MOR KO mice, with DA levels and the respective metabolites just in between the

midday and midnight levels of the WT mice (Figure 4A, MOR KO, midday, 153.35 ± 34.41, n=9; midnight, 180.06 ± 21.28, n=12; $F_{1,18}$=5.16, p=0.10; age, $F_{1,15}$=2.92, p=0.38; 4B, MOR KO, midday, 9.66 ± 1.87, n=9; midnight, 10.63 ± 1.38, n=12; $F_{1,18}$=2.24, p=0.33; age, $F_{1,15}$=4.93, p=0.43; 4C, MOR KO, midday, 17.65 ± 4.02, n=9; midnight, 17.08 ± 2.77, n=12; $F_{1,18}$=0.18, p=0.68; age, $F_{1,15}$=4.91, p=0.22; 4D, MOR KO, midday, 0.06 ± 0.01, n=9; midnight, 0.06 ± 0.01, n=12; $F_{1,18}$=1.63, p=0.30; age, $F_{1,15}$=0.08, p=0.78; 4E, MOR KO, midday, 0.07 ± 0.01, n=9; midnight, 0.06 ± 0.01, n=12; $F_{1,18}$=2.04, p=0.31; age, $F_{1,15}$=1.05, p=0.50; 4F, MOR KO, midday, 0.23 ± 0.03, n=9; midnight, 0.25 ± 0.02, n=12; $F_{1,18}$=1.79, p=0.31; age, $F_{1,15}$=0.57, p=0.56; all mixed model ANOVA).

Increased locomotion and thermal sensitivity in the MOR KO mice

RLS is characterized by a strong urge to move during inactivity, especially at night or at rest (Mansur, Castillo, Taub, & Bokhari, 2019). Previous phenotypic mouse models of RLS have shown altered activity levels (Clemens & Hochman, 2004; DeAndrade et al., 2012; Esteves, de Mello, Lancellotti, Natal, & Tufik, 2004; Meneely et al., 2018; Ondo, He, Rajasekaran, & Le, 2000; Silvani et al., 2015; Spieler et al., 2014). Here, to assess the activity levels of the MOR KO mice, we used a wheel running setup for consecutive five days under the normal 12 LD condition. The first three days are for accommodation and the data from the last two days (day 4, night 4, day 5, night 5) were included in the analysis. It should be noticed that RLS is a circadian component-involved disorder. Therefore, we analyzed the activity of mice during the light and the dark phase separately. Each phase contained data for two days or two nights. The day or night when the data were obtained was classified as "period" (Table 4). Differentiated night/day activity may reveal abnormalities in MOR KO mice not observed if only the overall movement is tracked (Samuels et al., 2017). We found that the voluntary activity was increased in the MOR KO mice during the light phase (period X genotype, p=0.07; Figure 5A, light phase, WT, n=5; KO, n=5, ES, 1.39, SE, 0.61, 95%CI, 0.19 and 2.59; Z=2.28, p=0.02; period, p=0.11; all GENMOD with a negative binomial distribution), especially at 6:00 AM (period X genotype, p=0.14; Figure 5A, right panel, WT, n=5; KO, n=5, ES, 3.94, SE, 0.62, 95%CI, 2.74 and 5.15; Z=6.41, p<0.01; period, p=0.21; all GENMOD with a negative binomial distribution) when the light just turned on and 5:00 PM (period X genotype, p=0.13; Figure 5A, right panel, WT, n=5; KO, n=5, ES, 4.42, SE, 0.96, 95%CI, 2.54 and 6.31; Z=4.61, p<0.01; period, p=0.40; all GENMOD with a negative binomial distribution), right before the dark phase. MOR KO mice had no statistically significant changes in activity levels during the dark phase, although the initial dark phase activity was numerically trending lower for MOR KO compared to WT and not showing the steep decline around midnight as seen for WT (period X genotype, p=0.83; Figure 5B, dark phase, WT, n=5; KO, n=5, ES, −0.23, SE, 0.24, 95%CI, −0.70 and 0.25; Z= −0.94, p=0.35; period, p=0.09; all GENMOD with a negative binomial distribution). Mice have an opposite circadian rhythm to human. They normally are resting or sleeping during the light phase and are active during the dark phase. Hence the data is consistent with clinical findings from patients. In addition, MOR KO mice showed decreased activity levels at 6:00 PM (period X genotype, p=0.83; Figure 5B, right panel, WT, n=5; KO, n=5, ES, −0.74, SE, 0.24, 95%CI, −1.20 and −0.28; Z=−3.15, p<0.01; period, p=0.21; all GENMOD with a negative binomial distribution), which can be considered as daytime sleepiness since the mice were over-active during the rest phase and did not get enough sleep, and at 3:00

AM (period X genotype, p=0.58; Figure 5B, right panel, WT, n=5; KO, n=5, ES, −1.36, SE, 0.61, 95%CI, −2.55 and −0.17; Z=−2.23, p=0.03; period, p=0.49; all GENMOD with a negative binomial distribution) and 4:00 AM (period X genotype, p=0.70; Figure 5B, right panel, WT, n=5; KO, n=5, ES, −1.55, SE, 0.67, 95%CI, −2.86 and −0.24; Z=−2.32, p=0.02; period, p=0.95; all GENMOD with a negative binomial distribution) in the dark phase, which is similar to the RLS patients. Whether the overall activity pattern of less steep increases and decreases, premature increase at the beginning of the active and delayed decrease before the rest phase, or both, are caused by the lack of a steep increase in DA levels in the KO mice (Figure 3A) remains to be investigated.

There were no significant changes in food and water intakes of the MOR KO mice compared with the WT mice, similar to previous observations (Samuels et al., 2017) (Supplementary Figure 2, food: WT, 4.72 ± 1.65, n=5; KO, 4.72 ± 1.15, n=5; $F_{1,7}$=0.00, p=1.00; water: WT, 4.19 ± 0.59, n=5; KO, 4.33 ± 0.60, n=5; $F_{1,7}$=0.42, p=0.54; all mixed model ANOVA). The result indicates that the increased activity during the light phase of the MOR KO was not influenced or caused by metabolic changes.

RLS patients show hypersensitivity to a pinprick as well as tactile hypoesthesia and dysesthesia to non-noxious cold stimuli (paradoxical heat sensation) (Stiasny-Kolster, Magerl, Oertel, Moller, & Treede, 2004; Stiasny-Kolster, Pfau, Oertel, Treede, & Magerl, 2013). Some of RLS patients exhibit hyperalgesia to blunt pressure and hyperaesthesia to vibration (Bachmann et al., 2010). Hence, we also tested the sensory system of the MOR KO using the tail-flick test (Table 5). Consistent with previous studies (Martin, Matifas, Maldonado, & Kieffer, 2003), the MOR KO mice showed increased sensitivity to the heat stimuli at the midday (age X genotype, p=0.72, weight X genotype, p=0.27; Figure 6A, WT, n=14; KO, n=14, ES, −0.30, SE, 0.13, 95%CI, −0.55 and −0.05; Z=−2.33, p=0.02; age, p=0.09, weight, p=0.03; all GENMOD with a gamma distribution). Next, we did the sensory test with another cohort of mice at midnight, at midday, and after the drug treatment, respectively. There were no significant interactions among age, genotype, and the time for testing (p=0.60, GENMOD with a gamma distribution). However, RLS patients show circadian variations of symptoms, and we were interested in determining whether MOR KO mice had sensory deficits at different time points. Hence the data were separately analyzed according to the time. We found that the sensory deficit of MOR KO mice only appear at midday (age X genotype, p=0.19, weight X genotype, p=0.23; Figure 6B, midday, WT, n=5; KO, n=6, ES, −0.42, SE, 0.11, 95%CI, −0.63 and −0.21; Z=−3.95, p<0.01; age, p=0.75, weight, p=0.25; all GENMOD with a gamma distribution; Supplementary Figure 3C, D), but not at the midnight (age X genotype, p=0.11, weight X genotype, p=0.06; Figure 6B, midnight, WT, n=5; KO, n=6, ES, −0.30, SE, 0.18, 95%CI, −0.65 and 0.05; Z=−1.70, p=0.09; age, p=0.53, weight, p=0.79; all GENMOD with a gamma distribution; Supplementary Figure 3A, B). One of the diagnostic criteria for human RLS states that the urge to move the legs and any accompanying unpleasant sensations begin or worsen during periods of rest or inactivity (Garcia Borreguero et al., 2017). The result indicates that the sensory deficit of the MOR KO mice has a circadian component akin to human RLS. Moreover, the decreased latency in response to the heat stimuli of MOR KO mice was rescued by the injection of ropinirole, a common dopaminergic treatment of RLS (age X genotype, p=0.98, weight X genotype, p=0.22; Figure 6B, after ropinirole, WT, n=5; KO,

n=6, ES, 0.17, SE, 0.10, 95%CI, −0.02 and 0.36; Z=1.78, p=0.08; age, p=0.22, weight, p=0.40; all GENMOD with a gamma distribution; Supplementary Figure 3E, F). The results are the same as what we found in the *Btbd9* KO mice (DeAndrade et al., 2012) and indicate a dopaminergic alteration in the MOR KO mice.

Discussion:

In the current study, male MOR KO mice had low serum iron, anemia and abnormal circadian variations in the dopaminergic and serotonergic systems partially comparable to those found in human RLS (Christopher J. Earley et al., 2017; Trotti, 2017). In addition, naloxonazine decreased the serum iron concentration in the WT mice, as observed in the male MOR KO mice. Finally, MOR KO mice had hyperactivity during the sleep period, analogous to that seen with human RLS, and sensory abnormalities also akin to those seen in human RLS (Trotti, 2017). There are limitations to this study. It is limited to male mice, and the link between the peripheral iron deficiency and central alterations of the DA system is not clear. However, we demonstrated that the endogenous mu opioid system plays an important role in iron homeostasis, anemia, circadian variations in the dopaminergic system, and the pathogenesis of RLS. It should be noticed that MOR KO mice will not serve as an RLS animal model since no genetic studies have linked MOR to RLS susceptibility, although the study investigated SNPs only with a frequency >1% and suggested that the 20 association signals found accounted for 60% of the SNP-based heritability (Schormair et al., 2017). Furthermore, functional changes of opioid receptor heterodimers formed between MOR other opioid receptor subtypes may contribute to the phenotype observed in MOR KO mice, which remains to be investigated.

Iron deficiency is thought to be the best-established chemical abnormality in RLS (Connor et al., 2017) and iron deficiency anemia is the most common type of anemia associated with RLS (Allen et al., 2013). The MOR KO mice showed a decreased level of iron and transferrin but elevated ferritin in the serum, and increased iron levels in spleen and liver. While in most patients with iron deficiency, serum ferritin is below the normal range, it is normal or high in patients with AI due to the stimulation of ferritin synthesis by both inflammation and macrophage iron loading. Inflammation may increase serum ferritin concentration independent from iron status (Kalantar-Zadeh, Rodriguez, & Humphreys, 2004). Previous mouse models of AI induced by bacteria injection or gene manipulation show a lower level of HB, decreased serum iron and increased iron in the liver (Gardenghi S, 2014; A. Kim et al., 2014; Roy et al., 2007). Microcytosis can be found in AI of long duration or in children, where there is an increased demand for iron for growth (Nemeth & Ganz, 2014). KO of MORs led to similar phenotypes. The endogenous opioid system has been found to be involved in the regulation of iron homeostasis and blood profile. Opiate drug abusers have higher levels of ferritin and a higher hematological index value in their blood samples compared with the control group (Verde Mendez, Diaz-Flores, Sanudo, Rodriguez Rodriguez, & Diaz Romero, 2003). Furthermore, heroin and opium dependent people have increased HCT, MCV and MCHC level (Haghpanah, Afarinesh, & Divsalar, 2010). Finally, a recent study demonstrated that chronic use of opioids not only alters all of the hematologic series but also triggers inflammatory processes in the brain and facilitates the release of histamine by activating the tyrosine kinases in the nonneuronal cells (Guzel,

Yazici, Yazici, & Erol, 2018), which can directly affect the dopamine system (Dong, Zhang, & Qian, 2014; Nishibori, Oishi, Itoh, & Saeki, 1985). Overall, the abnormal iron homeostasis in the MOR KO mice suggests a state of inflammation (Cappellini et al., 2017; Weiss & Goodnough, 2005) and the data from MOR KO mice is consistent with AI type of inflammation.

Interestingly, short-term blockade of MOR with an irreversibly binding MOR antagonist decreased the serum iron and showed numerical trends of alteration of ferritin and transferrin levels as seen in the MOR KO mice. It is unclear what mechanisms are involved in MOR KO mice that cause AI. Il-6 and other cytokines are established inducers of hepcidin, a 25 aa peptide hormone that results in endocytosis and proteolysis of the sole known cellular iron exporter, ferroportin. As a result, iron will be trapped in macrophages and iron-absorbing enterocytes. MOR has been found to have anti-inflammatory properties (Iwaszkiewicz, Schneider, & Hua, 2013; Stein, 2016). It is expressed on peripheral nociceptor terminals and immune cells (Stein, 2016). MOR mediated reduction in inflammation in two *in vivo* models of colitis can be reversed by naloxonazine (Philippe et al., 2003). Further, MOR KO mice have been reported to be vulnerable to inflammatory disease with a dramatic increase of inflammation, TNFα, Il-4 and INFγ mRNA levels and mortality in a colitis model (Philippe et al., 2003). However, whether MOR KO mice under control conditions show low grade chronic intestinal inflammation or increased Il-6 production remains elusive. In combination, our data indicate a relationship among MOR, inflammation, iron homeostasis and RLS.

Different from the triple KO mice (Lyu, DeAndrade, et al., 2019), MOR KO did not have decreased DOPAC to DA ratio, neither at the midday nor at midnight. In addition, our Western blot analyses with the MOR KO and their WT littermates did not show changes in the striatal D_1R, D_2R, and DAT protein levels, which is contrary to clinical findings showing decreased striatal D_2R or D_2R binding potential (Connor et al., 2009; C. J. Earley et al., 2013; Michaud, Soucy, Chabli, Lavigne, & Montplaisir, 2002), and alterations in the density of DAT (C. J. Earley et al., 2011; K. W. Kim et al., 2012). However, it is interesting that the circadian variations found in the dopaminergic and serotonergic systems in the WT mice were absent in the MOR KO mice. It has been found that extracellular DA concentration in the striatum is significantly increased during the dark phase compared with the light phase in rats (Hood et al., 2010; Smith, Olson, & Justice, 1992). A mouse study showed circadian fluctuations of DA, DOPAC, 3-MT, HVA, 5-HT and 5-HIAA levels in the striatum (Khaldy et al., 2002). Comparing the cerebrospinal fluids (CSFs) collected at 10:00 am and 10:00 pm, the researchers found opposite directions of changes in the HVA, 5-HIAA, 3-O-methyldopa (3-OMD) in a control group compared to the RLS patients (C. J. Earley, Hyland, & Allen, 2006). 3-OMD is one of the most important metabolites of L-DOPA, which is the precursor of DA. HVA and 5-HIAA are the main metabolites for DA and 5-HT, respectively. Moreover, the level of tetrahydrobiopterin (BH4), a cofactor for enzymes synthesizing neurotransmitters like DA and 5-HT, was significantly increased in a control group but decreased in RLS patients (C. J. Earley et al., 2006). These studies indicate RLS patients may have abnormal diurnal fluctuation of dopaminergic and serotonergic systems. Our result suggests that a disturbance in the circadian rhythm of the dopaminergic and serotonergic system may be critically involved in the pathogenesis of RLS.

The phenotypes of RLS patients are circadian-rhythm-dependent. The urge to move and uncomfortable sensations begin or worsen at night or inactivity (Garcia Borreguero et al., 2017). Like triple KO mice (Lyu, DeAndrade, et al., 2019), the MOR KO mice showed clear diurnal hyperactivity, with the increased interval counts appearing specifically during the rest phase, but not the active phase. MOR is involved in pain modulation, and morphine is a common drug used for analgesia (Nadal, La Porta, Andreea Bura, & Maldonado, 2013). It is not surprising that the MOR KO mice showed increased sensitivity to the heat stimuli in the tail-flick test, which is opposite to triple KO mice (Lyu, DeAndrade, et al., 2019). The interesting finding is that accompanying the rest-phase specific hyperactivity, the increased sensitivity of MOR KO also only occurred at midday, but not at midnight. Both of the phenotypes may be related to the disappearance of the normal fluctuations in the monoamine systems, which is supported by the fact that the sensory deficit could be reversed by the injection of a dopamine agonist. The results are similar to the phenotypes we observed in the *Btbd9* KO mice (DeAndrade et al., 2012) and confirm the involvement of circadian rhythm and the dopaminergic system in the model.

In summary, the anemia in human RLS is an iron deficiency anemia whereas the anemia observed in our MOR KO mice is characteristic of inflammatory anemia. In this sense, the previous triple KO mouse model is more characteristic of human RLS where we did observe anemia more similar to an iron deficiency anemia with the exception that transferrin levels were not elevated (Lyu, DeAndrade, et al., 2019). On the other hand, the MOR KO mouse model is more compatible with the high association RLS has with inflammatory disorders (Weinstock et al., 2012). This suggests that different opioid receptor subtypes may contribute either singly or in combination to produce different aspects of the RLS clinical spectrum. The fact that both our triple KO and MOR KO mouse models produced motor and sensory abnormalities akin to those of human RLS suggests that the MOR plays a key role in the mediation of the core features of RLS. This result is also compatible with the observation that all of the opiates that have been found to be successful in the treatment of human RLS are MOR agonists.

Supplementary Material

Refer to Web version on PubMed Central for supplementary material.

Other Acknowledgments:

References:

Allen RP, Auerbach S, Bahrain H, Auerbach M, & Earley CJ (2013). The prevalence and impact of restless legs syndrome on patients with iron deficiency anemia. Am J Hematol, 88(4), 261–264. doi:10.1002/ajh.23397 [PubMed: 23494945]

Allen RP, & Earley CJ (2007). The role of iron in restless legs syndrome. Mov Disord, 22 Suppl 18, S440–448. doi:10.1002/mds.21607 [PubMed: 17566122]

Allen RP, Picchietti DL, Garcia-Borreguero D, Ondo WG, Walters AS, Winkelman JW, … Lee HB (2014). Restless legs syndrome/Willis-Ekbom disease diagnostic criteria: updated International Restless Legs Syndrome Study Group (IRLSSG) consensus criteria--history, rationale, description, and significance. Sleep Med, 15(8), 860–873. doi:10.1016/j.sleep.2014.03.025 [PubMed: 25023924]

Anderson GJ, & Frazer DM (2017). Current understanding of iron homeostasis. Am J Clin Nutr, 106(Suppl 6), 1559s-1566s. doi:10.3945/ajcn.117.155804 [PubMed: 29070551]

Bachmann CG, Rolke R, Scheidt U, Stadelmann C, Sommer M, Pavlakovic G, … Paulus W (2010). Thermal hypoaesthesia differentiates secondary restless legs syndrome associated with small fibre neuropathy from primary restless legs syndrome. Brain, 133(Pt 3), 762–770. doi:10.1093/brain/awq026 [PubMed: 20194142]

Bachmanov AA, Reed DR, Beauchamp GK, & Tordoff MG (2002). Food Intake, Water Intake, and Drinking Spout Side Preference of 28 Mouse Strains. Behav Genet, 32(6), 435–443. [PubMed: 12467341]

Cappellini MD, Comin-Colet J, de Francisco A, Dignass A, Doehner W, Lam CS, … Musallam KM (2017). Iron deficiency across chronic inflammatory conditions: International expert opinion on definition, diagnosis, and management. Am J Hematol, 92(10), 1068–1078. doi:10.1002/ajh.24820 [PubMed: 28612425]

Clemens S, & Hochman S (2004). Conversion of the modulatory actions of dopamine on spinal reflexes from depression to facilitation in D3 receptor knock-out mice. J Neurosci, 24(50), 11337–11345. doi:10.1523/jneurosci.3698-04.2004 [PubMed: 15601940]

Connor JR, Patton S, Oexle K, & Allen R (2017). Iron and restless legs syndrome: Treatment, genetics and pathophysiology. Sleep Med, 31, 61–70. doi:10.1016/j.sleep.2016.07.028 [PubMed: 28057495]

Connor JR, Wang XS, Allen RP, Beard JL, Wiesinger JA, Felt BT, & Earley CJ (2009). Altered dopaminergic profile in the putamen and substantia nigra in restless leg syndrome. Brain, 132(Pt 9), 2403–2412. doi:10.1093/brain/awp125 [PubMed: 19467991]

DeAndrade MP, Johnson RL Jr., Unger EL, Zhang L, van Groen T, Gamble KL, & Li Y (2012). Motor restlessness, sleep disturbances, thermal sensory alterations and elevated serum iron levels in Btbd9 mutant mice. Hum Mol Genet, 21(18), 3984–3992. doi:10.1093/hmg/dds221 [PubMed: 22678064]

Dong H, Zhang X, & Qian Y (2014). Mast Cells and Neuroinflammation. In Med Sci Monit Basic Res (Vol. 20, pp. 200–206).

Earley CJ, Hyland K, & Allen RP (2006). Circadian changes in CSF dopaminergic measures in restless legs syndrome. Sleep Med, 7(3), 263–268. doi:10.1016/j.sleep.2005.09.006 [PubMed: 16564215]

Earley CJ, Kuwabara H, Wong DF, Gamaldo C, Salas R, Brasic J, … Allen RP (2011). The dopamine transporter is decreased in the striatum of subjects with restless legs syndrome. Sleep, 34(3), 341–347. [PubMed: 21358851]

Earley CJ, Kuwabara H, Wong DF, Gamaldo C, Salas RE, Brasic JR, … Allen RP (2013). Increased synaptic dopamine in the putamen in restless legs syndrome. Sleep, 36(1), 51–57. doi:10.5665/sleep.2300 [PubMed: 23288971]

Earley CJ, Uhl GR, Clemens S, & Ferré S (2017). Connectome and molecular pharmacological differences in the dopaminergic system in restless legs syndrome (RLS): plastic changes and neuroadaptations that may contribute to augmentation. Sleep Medicine, 31, 71–77. doi:10.1016/j.sleep.2016.06.003 [PubMed: 27539027]

Esteves AM, de Mello MT, Lancellotti CL, Natal CL, & Tufik S (2004). Occurrence of limb movement during sleep in rats with spinal cord injury. Brain Res, 1017(1–2), 32–38. doi:10.1016/j.brainres.2004.05.021 [PubMed: 15261096]

Garcia Borreguero D, Winkelmann J, & Allen RP (2017). Introduction: Towards a better understanding of the science of RLS/WED. Sleep Med, 31, 1–2. doi:10.1016/j.sleep.2016.10.007 [PubMed: 27894926]

Gardenghi S RT, Meloni A, Casu C, Crielaard BJ, Bystrom LM, Greenberg-Kushnir N, Sasu BJ, Cooke KS, Rivella S (2014). Distinct roles for hepcidin and interleukin-6 in the recovery from

anemia in mice injected with heat-killed Brucella abortus. blood, 123(8), 1137–1145. [PubMed: 24357729]

Guzel D, Yazici AB, Yazici E, & Erol A (2018). Evaluation of Immunomodulatory and Hematologic Cell Outcome in Heroin/Opioid Addicts. J Addict, 2018, 2036145. doi:10.1155/2018/2036145 [PubMed: 30631635]

Haghpanah T, Afarinesh M, & Divsalar K (2010). A review on hematological factors in opioid-dependent people (opium and heroin) after the withdrawal period. Addict Health, 2(1–2), 9–16. [PubMed: 24494095]

Hastka J, Lasserre JJ, Schwarzbeck A, Strauch M, & Hehlmann R (1993). Zinc protoporphyrin in anemia of chronic disorders. Blood, 81(5), 1200–1204. [PubMed: 8443380]

Hood S, Cassidy P, Cossette MP, Weigl Y, Verwey M, Robinson B, … Amir S (2010). Endogenous dopamine regulates the rhythm of expression of the clock protein PER2 in the rat dorsal striatum via daily activation of D2 dopamine receptors. J Neurosci, 30(42), 14046–14058. doi:10.1523/jneurosci.2128-10.2010 [PubMed: 20962226]

Iwaszkiewicz KS, Schneider JJ, & Hua S (2013). Targeting peripheral opioid receptors to promote analgesic and anti-inflammatory actions. Front Pharmacol, 4, 132. doi:10.3389/fphar.2013.00132 [PubMed: 24167491]

Kalantar-Zadeh K, Rodriguez RA, & Humphreys MH (2004). Association between serum ferritin and measures of inflammation, nutrition and iron in haemodialysis patients. Nephrol Dial Transplant, 19(1), 141–149. [PubMed: 14671049]

Kell DB, & Pretorius E (2014). Serum ferritin is an important inflammatory disease marker, as it is mainly a leakage product from damaged cells. Metallomics, 6(4), 748–773. doi:10.1039/c3mt00347g [PubMed: 24549403]

Khaldy H, Leon J, Escames G, Bikjdaouene L, Garcia JJ, & Acuna-Castroviejo D (2002). Circadian rhythms of dopamine and dihydroxyphenyl acetic acid in the mouse striatum: effects of pinealectomy and of melatonin treatment. Neuroendocrinology, 75(3), 201–208. doi:10.1159/000048238 [PubMed: 11914592]

Kim A, Fung E, Parikh SG, Valore EV, Gabayan V, Nemeth E, & Ganz T (2014). A mouse model of anemia of inflammation: complex pathogenesis with partial dependence on hepcidin. Blood, 123(8), 1129–1136. doi:10.1182/blood-2013-08-521419 [PubMed: 24357728]

Kim KW, Jhoo JH, Lee SB, Lee SD, Kim TH, Kim SE, … Yoon IY (2012). Increased striatal dopamine transporter density in moderately severe old restless legs syndrome patients. Eur J Neurol, 19(9), 1213–1218. doi:10.1111/j.1468-1331.2012.03705.x [PubMed: 22435397]

Lyu S, DeAndrade MP, Mueller S, Oksche A, Walters AS, & Li Y (2019). Hyperactivity, dopaminergic abnormalities, iron deficiency and anemia in an in vivo opioid receptors knockout mouse: Implications for the Restless Legs Syndrome. Behav Brain Res, 10.1016/j.bbr.2019.112123. doi:10.1016/j.bbr.2019.112123

Lyu S, Xing H, DeAndrade MP, Liu Y, Perez PD, Yokoi F, … Li Y (2019). The role of BTBD9 in striatum and restless legs syndrome. eNeuro. doi:10.1523/eneuro.0277-19.2019

Lyu S, Xing H, DeAndrade MP, Perez PD, Zhang K, Liu Y, … Li Y (2019). The role of BTBD9 in the cerebral cortex and the pathogenesis of restless legs syndrome. Experimental Neurology. doi:10.1016/j.expneurol.2019.113111

Mansur A, Castillo PR, Taub LFM, & Bokhari SRA (2019). Restless Leg Syndrome. In StatPearls. Treasure Island (FL): StatPearls PublishingStatPearls Publishing LLC.

Martin M, Matifas A, Maldonado R, & Kieffer BL (2003). Acute antinociceptive responses in single and combinatorial opioid receptor knockout mice: distinct mu, delta and kappa tones. Eur J Neurosci, 17(4), 701–708. [PubMed: 12603260]

Meneely S, Dinkins M-L, Kassai M, Lyu S, Liu Y, Lin C-T, … Clemens S (2018). Differential dopamine D1 and D3 receptor modulation and expression in the spinal cord of two mouse models of Restless Legs Syndrome. Frontiers in Behavioral Neuroscience, 12. doi:10.3389/fnbeh.2018.00199 [PubMed: 29441002]

Michaud M, Soucy JP, Chabli A, Lavigne G, & Montplaisir J (2002). SPECT imaging of striatal pre- and postsynaptic dopaminergic status in restless legs syndrome with periodic leg movements in sleep. J Neurol, 249(2), 164–170. [PubMed: 11985381]

Nadal X, La Porta C, Andreea Bura S, & Maldonado R (2013). Involvement of the opioid and cannabinoid systems in pain control: new insights from knockout studies. Eur J Pharmacol, 716(1–3), 142–157. doi:10.1016/j.ejphar.2013.01.077 [PubMed: 23523475]

Nemeth E, & Ganz T (2014). Anemia of Inflammation. Hematol Oncol Clin North Am, 28(4), 671–681. doi:10.1016/j.hoc.2014.04.005 [PubMed: 25064707]

Nishibori M, Oishi R, Itoh Y, & Saeki K (1985). Morphine-induced changes in histamine dynamics in mouse brain. J Neurochem, 45(3), 719–724. [PubMed: 4031857]

Ondo WG, He Y, Rajasekaran S, & Le WD (2000). Clinical correlates of 6-hydroxydopamine injections into A11 dopaminergic neurons in rats: a possible model for restless legs syndrome. Mov Disord, 15(1), 154–158. [PubMed: 10634257]

Philippe D, Dubuquoy L, Groux H, Brun V, Chuoï-Mariot MTV, Gaveriaux-Ruff C, … Desreumaux P (2003). Anti-inflammatory properties of the μ opioid receptor support its use in the treatment of colon inflammation. In J Clin Invest (Vol. 111, pp. 1329–1338).

Rahimdel AG, Ayatollahi P, Zeinali A, Mehrabanian N, & Mellat-Ardekani A (2012). The Effect of Selenium Administration on Restless Leg Syndrome Treatment. Iran Red Crescent Med J, 14(1), 14–19. [PubMed: 22737548]

Roy CN, Mak HH, Akpan I, Losyev G, Zurakowski D, & Andrews NC (2007). Hepcidin antimicrobial peptide transgenic mice exhibit features of the anemia of inflammation. Blood, 109(9), 4038–4044. doi:10.1182/blood-2006-10-051755 [PubMed: 17218383]

Samuels BA, Nautiyal KM, Kruegel AC, Levinstein MR, Magalong VM, Gassaway MM, … Hen R (2017). The Behavioral Effects of the Antidepressant Tianeptine Require the Mu-Opioid Receptor. Neuropsychopharmacology, 42(10), 2052–2063. doi:10.1038/npp.2017.60 [PubMed: 28303899]

Schormair B, Zhao C, Bell S, Tilch E, Salminen AV, Putz B, … Winkelmann J (2017). Identification of novel risk loci for restless legs syndrome in genome-wide association studies in individuals of European ancestry: a meta-analysis. Lancet Neurol, 16(11), 898–907. doi:10.1016/s1474-4422(17)30327-7 [PubMed: 29029846]

Silvani A, Lo Martire V, Salvade A, Bastianini S, Ferri R, Berteotti C, … Manconi M (2015). Physiological time structure of the tibialis anterior motor activity during sleep in mice, rats and humans. J Sleep Res, 24(6), 695–701. doi:10.1111/jsr.12319 [PubMed: 26118726]

Smith AD, Olson RJ, & Justice JB Jr. (1992). Quantitative microdialysis of dopamine in the striatum: effect of circadian variation. J Neurosci Methods, 44(1), 33–41. [PubMed: 1279321]

Spieler D, Kaffe M, Knauf F, Bessa J, Tena JJ, Giesert F, … Winkelmann J (2014). Restless Legs Syndrome-associated intronic common variant in Meis1 alters enhancer function in the developing telencephalon. Genome Res, 24(4), 592–603. doi:10.1101/gr.166751.113 [PubMed: 24642863]

Stein C (2016). Opioid Receptors. Annu Rev Med, 67, 433–451. doi:10.1146/annurev-med-062613-093100 [PubMed: 26332001]

Stiasny-Kolster K, Magerl W, Oertel WH, Moller JC, & Treede RD (2004). Static mechanical hyperalgesia without dynamic tactile allodynia in patients with restless legs syndrome. Brain, 127(Pt 4), 773–782. doi:10.1093/brain/awh079 [PubMed: 14985260]

Stiasny-Kolster K, Pfau DB, Oertel WH, Treede RD, & Magerl W (2013). Hyperalgesia and functional sensory loss in restless legs syndrome. Pain, 154(8), 1457–1463. doi:10.1016/j.pain.2013.05.007 [PubMed: 23707286]

Sun YM, Hoang T, Neubauer JA, & Walters AS (2011). Opioids protect against substantia nigra cell degeneration under conditions of iron deprivation: a mechanism of possible relevance to the Restless Legs Syndrome (RLS) and Parkinson's disease. J Neurol Sci, 304(1–2), 93–101. doi:10.1016/j.jns.2011.02.003 [PubMed: 21376342]

Torrance JD, & Bothwell TH (1968). A simple technique for measuring storage iron concentrations in formalinised liver samples. S Afr J Med Sci, 33(1), 9–11. [PubMed: 5676884]

Trenkwalder C, Benes H, Grote L, Garcia-Borreguero D, Hogl B, Hopp M, … Kohnen R (2013). Prolonged release oxycodone-naloxone for treatment of severe restless legs syndrome after failure of previous treatment: a double-blind, randomised, placebo-controlled trial with an open-label extension. Lancet Neurol, 12(12), 1141–1150. doi:10.1016/s1474-4422(13)70239-4 [PubMed: 24140442]

Trotti LM (2017). Restless Legs Syndrome and Sleep-Related Movement Disorders. Continuum (Minneap Minn), 23(4, Sleep Neurology), 1005–1016. doi:10.1212/con.0000000000000488 [PubMed: 28777173]

Trotti LM, & Becker LA (2019). Iron for the treatment of restless legs syndrome. Cochrane Database Syst Rev, 1, Cd007834. doi:10.1002/14651858.CD007834.pub3 [PubMed: 30609006]

Ulfberg J, Stehlik R, & Mitchell U (2016). Treatment of restless legs syndrome/Willis-Ekbom disease with selenium. Iran J Neurol, 15(4), 235–236. [PubMed: 28435634]

Verde Mendez CM, Diaz-Flores JF, Sanudo RI, Rodriguez Rodriguez EM, & Diaz Romero C (2003). [Haematologic parameters in opiate addicts]. Nutr Hosp, 18(6), 358–365. [PubMed: 14682184]

von Spiczak S, Whone AL, Hammers A, Asselin MC, Turkheimer F, Tings T, … Brooks DJ (2005). The role of opioids in restless legs syndrome: an [11C]diprenorphine PET study. Brain, 128(Pt 4), 906–917. doi:10.1093/brain/awh441 [PubMed: 15728657]

Walters AS, Ondo WG, Zhu W, & Le W (2009). Does the endogenous opiate system play a role in the Restless Legs Syndrome? A pilot post-mortem study. J Neurol Sci, 279(1–2), 62–65. doi:10.1016/j.jns.2008.12.022 [PubMed: 19167016]

Walters AS, Patton S, Connor J, Bagai K, Anderson A, Bowman A, & Aschner M (2016). What about the other body metals in RLS?: Preliminary evidence for an increase in Zinc in Restless Legs Syndrome. Sleep, 39(Suppl), A229.

Wanner V, Garcia Malo C, Romero S, Cano-Pumarega I, & Garcia-Borreguero D (2019). Non-dopaminergic vs. dopaminergic treatment options in restless legs syndrome. Adv Pharmacol, 84, 187–205. doi:10.1016/bs.apha.2019.02.003 [PubMed: 31229171]

Weinstock LB, Walters AS, & Paueksakon P (2012). Restless legs syndrome--theoretical roles of inflammatory and immune mechanisms. Sleep Med Rev, 16(4), 341–354. doi:10.1016/j.smrv.2011.09.003 [PubMed: 22258033]

Weiss G, & Goodnough LT (2005). Anemia of chronic disease. N Engl J Med, 352(10), 1011–1023. doi:10.1056/NEJMra041809 [PubMed: 15758012]

Wessling-Resnick M (2010). Iron Homeostasis and the Inflammatory Response. Annu Rev Nutr, 30, 105–122. doi:10.1146/annurev.nutr.012809.104804 [PubMed: 20420524]

Yokoi F, Dang MT, Liu J, Gandre JR, Kwon K, Yuen R, & Li Y (2015). Decreased dopamine receptor 1 activity and impaired motor-skill transfer in Dyt1 DeltaGAG heterozygous knock-in mice. Behav Brain Res, 279, 202–210. doi:10.1016/j.bbr.2014.11.037 [PubMed: 25451552]

Significance statement:

RLS is a common sensorimotor disorder affecting up to 10% of the population, and its pathophysiology is largely unknown. Previous human, triple opioid receptors KO mouse, and cell culture studies indicate an involvement of the endogenous opioid system in RLS. The current study extended the study with triple KO mice to the mu opioid receptor subtype. By probing the behavioral and biochemical parameters relevant to RLS with MOR KO mice, we uncovered potential novel mechanisms for the development of human RLS, which are anemia of inflammation and loss of circadian variations in monoamine systems.
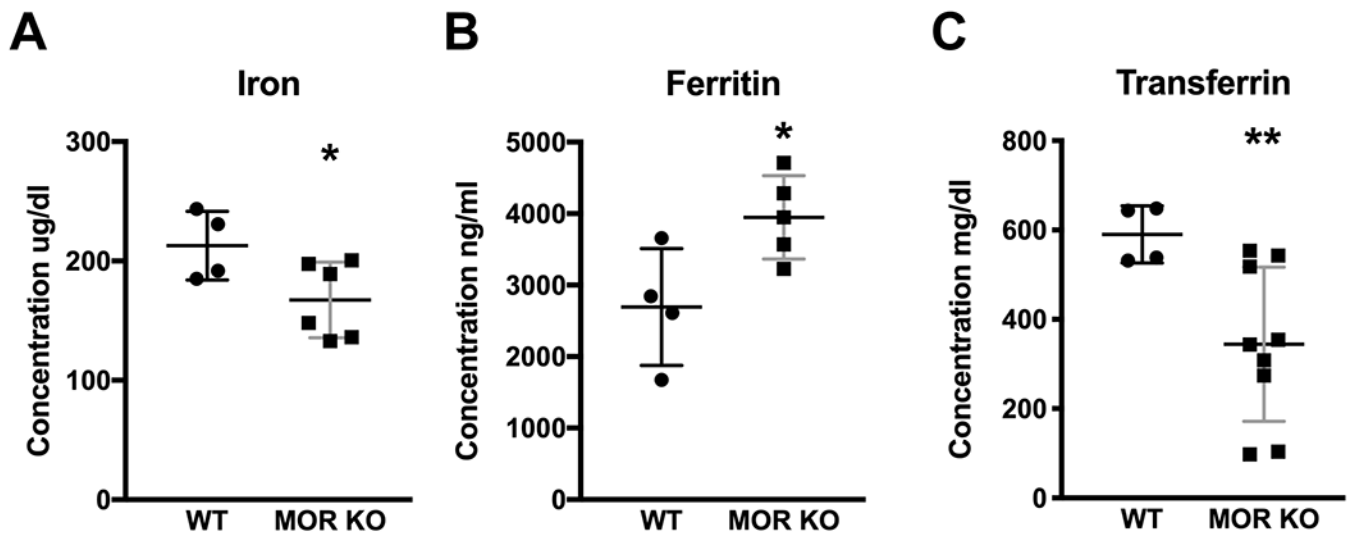
Figure 1.
Concentrations of iron, ferritin and transferrin in the serum. (A) The MOR KO mice (n=6) showed a decreased level of iron in serum compared with the WT (n=4). (B) The MOR KO mice (n=6) had an increased level of ferritin in serum compared with the WT (n=4). (C) The MOR KO (n=9) had a decreased level of transferrin in their serum compared with WT littermates (n=4). Data were analyzed by the unpaired Student's t-test and are presented as the means plus the standard deviations (SDs). * p 0.05; ** $p<0.01$. Only males were used in the experiment.
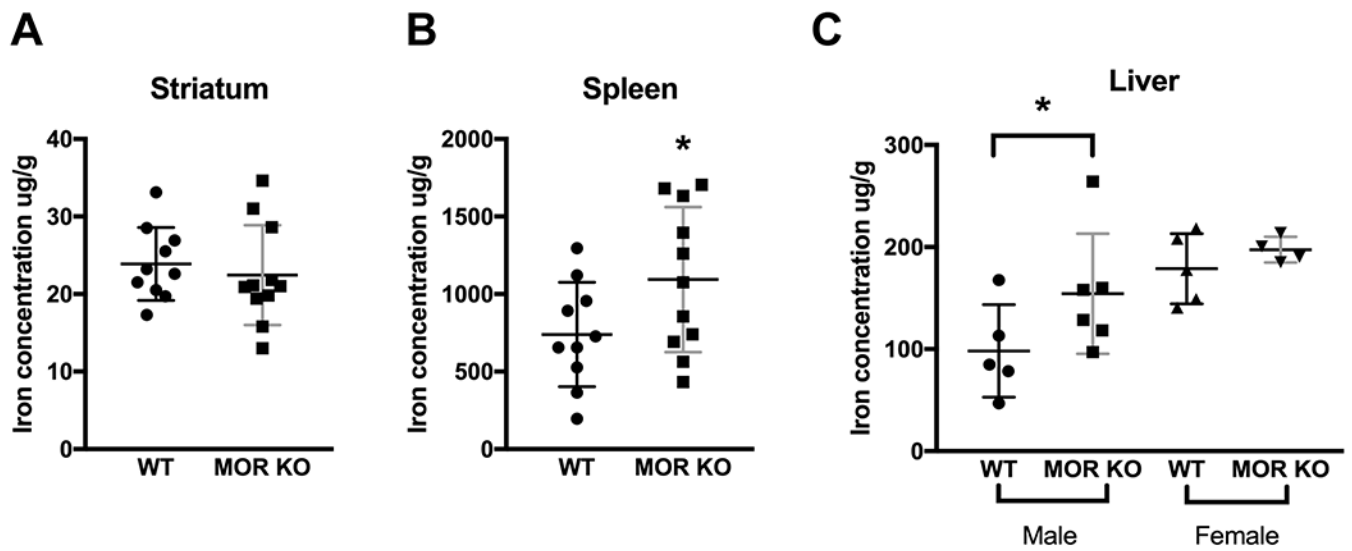
Figure 2.
Iron concentrations in tissues. (A) No change in the striatal iron level in the MOR KO mice (n=11) compared with the WTs (n=10). (B) The MOR KO mice (n=11) showed an increased iron level in the spleen compared with the WTs (n=10). (C) Male MOR KO mice (n=6), had an increased level of iron in their livers compared with the WT littermates (n= 5). Data were analyzed by the mixed model ANOVA and are presented as the means plus the SDs. * p 0.05. Both male and female were used in the experiment. Detailed analyses are in Table 2.
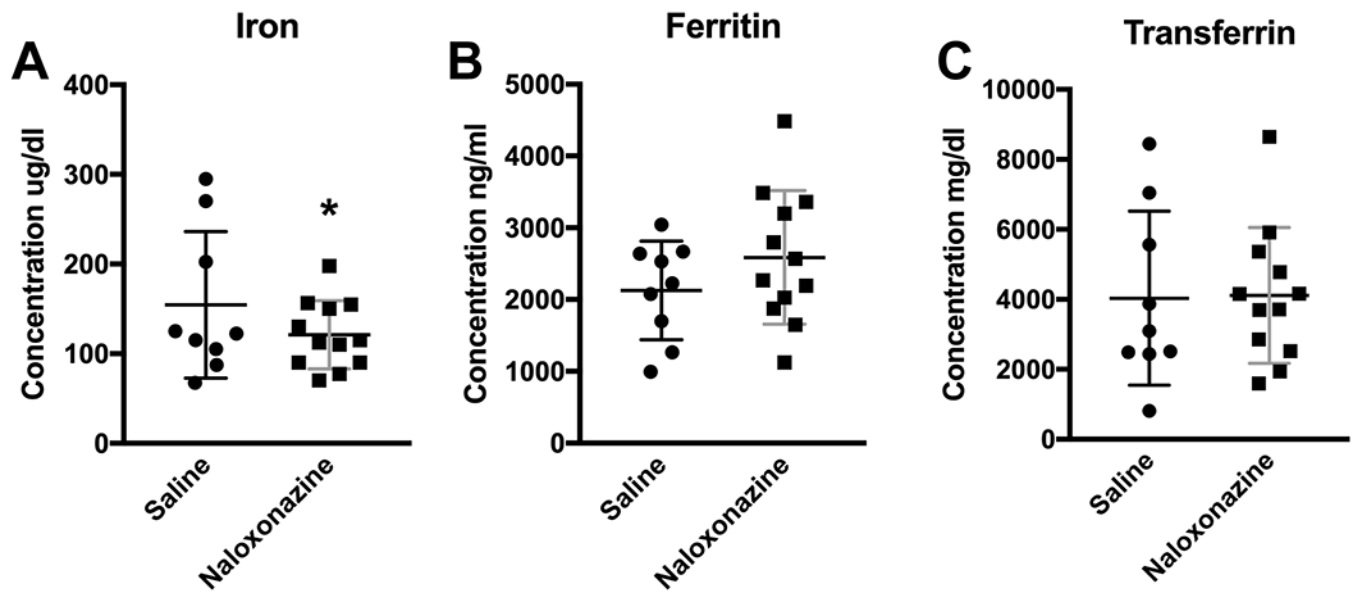
Figure 3.

Iron concentrations in serum of mice injected with naloxonazine (n=12) or saline (n=9). (A) The iron level decreased with naloxonazine injection. (B, C) Ferritin and transferrin levels did not have significant changes after the drug injection. Data in Figure 3A were analyzed by the GENMOD with a gamma distribution. Data in B and C were analyzed by the mixed model ANOVA. Scatter plots represent the means plus the SDs. * p 0.05. Only males were used in the experiment.

Figure 4.

Circadian variations in the striatal dopaminergic and serotonergic systems. (A, B, C) DA, DOPAC, and HVA levels increased in the WT but did not change in the MOR KO mice, during the night (WT, n=10; KO, n=12) compared with the day (WT, n=8; KO, n=9). (D, E) The ratio of DOPAC to DA or 3-MT to DA decreased in the WT during the night but did not change in the MOR KO mice compared with the ratios of the day. (F) The ratio of 5-HIAA to 5-HT increased in the WT mice during the night compared with the day but did not change in the MOR KO mice. Data were analyzed by the mixed model ANOVA and are presented as the means plus the SDs. DOPAC, 3,4-Dihydroxyphenylacetic acid; DA, Dopamine; HVA, Homovanillic acid; 3-MT, 3-Methoxytyramine; 5-HIAA, 5-Hydroxyindoleacetic acid; 5-HT, Serotonin. Bars represent the means plus the SDs. * p 0.05; ** p<0.01. p values have been adjusted for multiple comparisons using the Benjamini-Hochberg-Yekutieli false discovery rate [FDR ($p < 0.05$)]. Only males were used in the experiment. Detailed analyses are in Table 3.
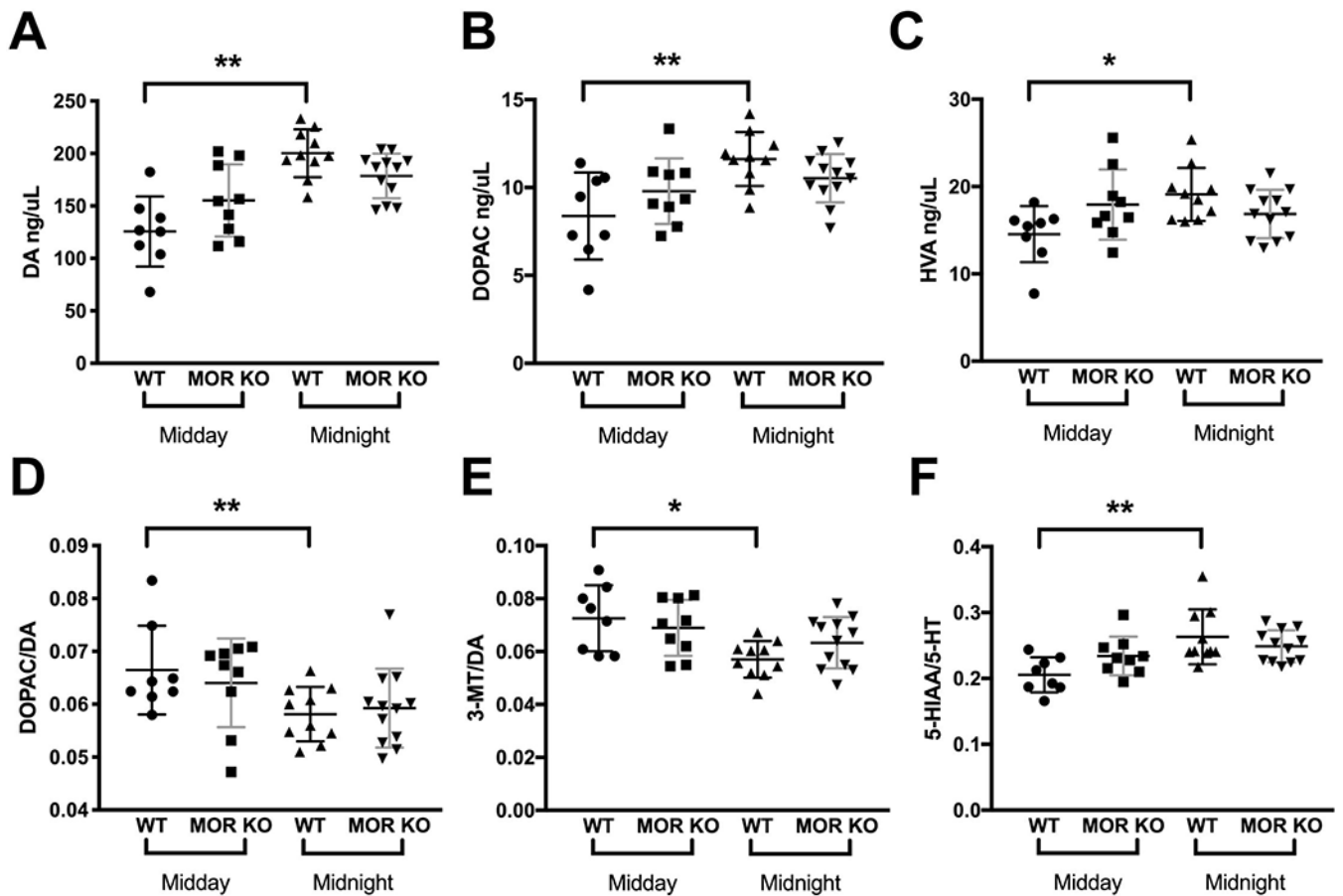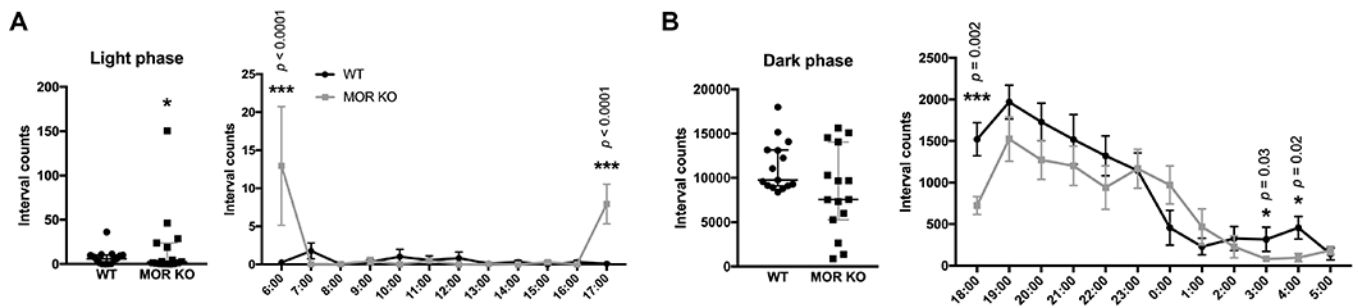
Figure 5.
Wheel running test. (A) The MOR KO mice (n=5) had a significant increase in voluntary activity during the light phase (2 days) compared with the WT littermates (n=5). The hourly activity is presented next to the scatter plot. (B) MOR KO mice (n=5) did not have significant changes in the voluntary activity during the dark phase (2 nights) compared with the WT littermates (n=5). However, MOR KO mice had significantly lower activity levels at 6:00 PM 3:00 AM and 4:00 AM. Data were analyzed by the GENMOD with a negative binominal distribution and are presented as medians with 95% confidence intervals (CIs). The hourly activity levels are presented as means plus the SDs. Significant *p* values are marked above the individual time point. * *p* 0.05; ** *p*<0.01. Only males were used in the experiment. Detailed analyses are in Table 4.
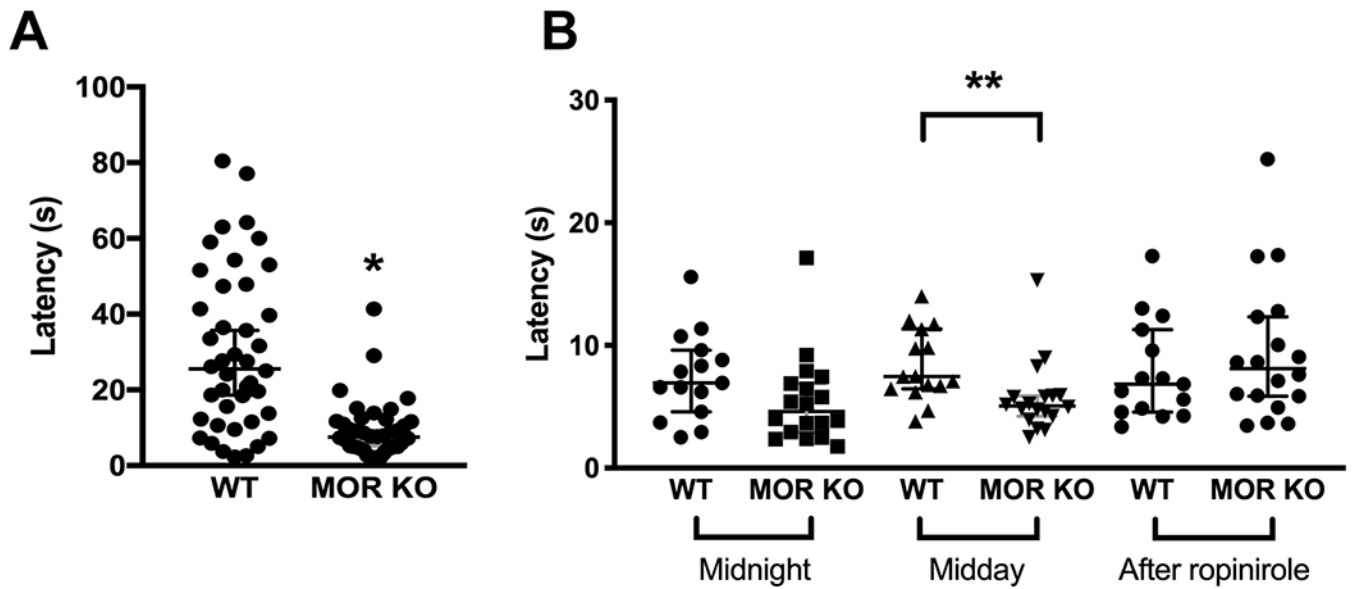
Figure 6.
Tail-flick test. (A) The MOR KO mice (n=14, 3 repeats) had decreased latency in response to the heat stimuli compared with the WT mice (n=14, 3 repeats). (B) The increased pain sensitivity of the MOR KO mice (n=6, 3 repeats) compared to the WTs (n=5, 3 repeats) only appeared at midday, but not at midnight. After the drug injection, there was no difference between the two groups. Data were analyzed by the GENMOD with a gamma distribution and are presented as medians with 95% CIs. * p 0.05; ** p<0.01. Only males were used in the experiment. Each mouse was tested three times. Each time was coded as trial1, trial2, and trial3, respectively. When data was processed, the "trial" was treated as a repeated measurement and nested under the Animal_ID. Detailed analyses are in Table 5. Age and weight were considered as continuous variables, and their relationships were further analyzed in Supplementary Figure 3.

Table 1.

Results of the Complete Blood Count (CBC) test.

CBC test Results	WT (n=4)		MOR KO (n=11)		$F_{1,12}$ values	p values
	Mean	SD	Mean	SD		
RBC M/uL	9.91	±1.12	8.01	1.03	5.74	0.03 *
HB g/dL	12.26	±1.09	9.77	±1.52	5.42	0.04 *
HCT %	40.21	±4.23	32.26	±4.69	5.18	0.04 *
PLT K/uL	583.50	±353.51	387.64	365.46	2.53	0.06
MCV fL	40.83	±0.64	40.48	±0.88	0.31	0.59
MCH pg	12.41	±0.55	12.18	±0.52	0.34	0.57
MCHC g/dL	30.49	±1.45	30.10	±1.09	0.19	0.67
RDW %	18.47	±1.16	17.22	±1.09	2.76	0.12
MPV fL	4.43	±0.63	3.25	±0.81	4.13	0.06
PDW %	26.36	±3.50	33.06	±5.42	3.18	0.10
Microcytic or hypochromic RBC	0 out of 4		5 out of 9			0.10

The values of each parameter are presented in means ± SDs. The p-values were calculated by mixed model ANOVA. RBC, red blood cells; HB, hemoglobin; HCT, hematocrit; PLT, platelet count; MCV, mean corpuscular volume; MCH, mean corpuscular hemoglobin; MCHC, mean corpuscular hemoglobin concentration; RDW, red blood cell distribution width; MPV, mean platelet volume; PDW, platelet distribution width. M: million; K: thousand; WT, wild-type mice. MOR KO, mu opioid receptor knockout mice.

*
p 0.05.

Table 2.

Iron concentrations in striatum, spleen, and liver.

Tissues	WT (n=10)	MOR KO (n=11)	Sex X Genotype	Sex	Genotype
Striatum	23.87 ± 4.70	23.16 ± 6.46	$F_{1,17}=0.59$ $p=0.45$	$F_{1,18}=5.10$ $p=0.04$*	$F_{1,18}=0.10$ $p=0.76$
Spleen	739.20 ± 467.63	1118.70 ± 336.62	$F_{1,17}=0.01$ $p=0.91$	$F_{1,18}=1.00$ $p=0.33$	$F_{1,18}=4.38$ $p=0.05$*

	Female				Male				Sex X Genotype	Sex	Genotype
	WT (n=5)	MOR KO (n=4)	$F_{1,7}$	p	WT (n=5)	MOR KO (n=6)	$F_{1,9}$	p			
Liver	178.75±34.46	197.46±12.66	1.04	0.53	98.16±45.37	154.34±58.89	3.03	0.05*	$F_{1,16}=0.89$ $p=0.36$	$F_{1,17}=9.92$ $p<0.01$**	$F_{1,17}=4.01$ $p=0.06$

The values of each parameter are presented in means ± SDs and p-values for interactions (Sex X Genotype) were calculated by mixed model ANOVA. The p-values for sex and genotype were calculated by mixed model ANOVA with the interaction removed. The p-values for the genotype of each sex were calculated by mixed model ANOVA using BY commend.

*
p 0.05;

**
$p<0.01$. WT, wild-type mice. MOR KO, mu opioid receptor knockout mice.

Table 3.

Monoamine levels in the striatum.

Monoamines and Metabolites	WT (n=18)				MOR KO (n=21)				Genotype X Time
	Midday (n=8)	Midnight (n=10)	Age	Time	Midday (n=9)	Midnight (n=12)	Age	Time	
NA	7.20 ± 2.06	3.86 ± 1.04	$F_{1,15}=1.56$ $p=0.51$	$F_{1,15}=20.16$ $p<0.01^{**}$	6.88 ± 1.62	4.20 ± 1.42	$F_{1,18}=1.66$ $p=0.59$	$F_{1,18}=16.29$ $p<0.01^{**}$	$F_{1,34}=0.46$ $p=0.50$
DOPAC	8.59 ± 2.47	11.46 ± 1.53	$F_{1,15}=7.26$ $p=0.10$	$F_{1,15}=12.37$ $p<0.01^{**}$	9.66 ± 1.87	10.63 ± 1.38	$F_{1,18}=4.93$ $p=0.43$	$F_{1,18}=2.24$ $p=0.33$	$F_{1,34}=3.45$ $p=0.07$
DA	127.18 ± 33.45	199.01 ± 22.78	$F_{1,15}=1.52$ $p=0.43$	$F_{1,15}=29.43$ $p<0.01^{**}$	153.35 ± 34.41	180.06 ± 21.28	$F_{1,18}=2.92$ $p=0.38$	$F_{1,18}=5.16$ $p=0.10$	$F_{1,34}=6.72$ $p=0.01^{*}$
5-HIAA	4.53 ± 0.83	5.24 ± 1.18	$F_{1,15}=1.10$ $p=0.76$	$F_{1,15}=1.91$ $p=0.19$	4.98 ± 0.93	4.66 ± 0.87	$F_{1,18}=1.31$ $p=0.59$	$F_{1,18}=0.64$ $p=0.47$	$F_{1,34}=2.63$ $p=0.11$
HVA	14.76 ± 3.21	18.94 ± 3.04	$F_{1,15}=2.42$ $p=0.39$	$F_{1,15}=8.46$ $p=0.02^{*}$	17.65 ± 4.02	17.08 ± 2.77	$F_{1,18}=4.91$ $p=0.22$	$F_{1,18}=0.18$ $p=0.68$	$F_{1,34}=5.86$ $p=0.02^{*}$
5-HT	22.39 ± 3.94	19.62 ± 1.77	$F_{1,15}=3.78$ $p=0.26$	$F_{1,15}=4.57$ $p=0.06$	21.31 ± 2.63	18.60 ± 2.11	$F_{1,18}=1.24$ $p=0.51$	$F_{1,18}=6.76$ $p=0.07$	$F_{1,34}=0.00$ $p=0.98$
3-MT	9.09 ± 2.38	11.37 ± 1.77	$F_{1,15}=0.20$ $p=0.73$	$F_{1,15}=5.01$ $p=0.05^{*}$	10.45 ± 2.09	11.42 ± 2.46	$F_{1,18}=0.73$ $p=0.56$	$F_{1,18}=0.87$ $p=0.44$	$F_{1,34}=0.81$ $p=0.37$
DOPAC/DA	0.07 ± 0.01	0.06 ± 0.01	$F_{1,15}=13.17$ $p=0.03^{*}$	$F_{1,15}=16.11$ $p<0.01^{**}$	0.06 ± 0.01	0.06 ± 0.01	$F_{1,18}=0.08$ $p=0.78$	$F_{1,18}=1.63$ $p=0.30$	$F_{1,34}=1.22$ $p=0.28$
HVA/DA	0.12 ± 0.01	0.10 ± 0.01	$F_{1,15}=0.32$ $p=0.71$	$F_{1,15}=15.82$ $p<0.01^{**}$	0.12 ± 0.01	0.10 ± 0.01	$F_{1,18}=0.45$ $p=0.56$	$F_{1,18}=16.33$ $p<0.01^{**}$	$F_{1,34}=0.01$ $p=0.94$
5-HIAA/5-HT	0.20 ± 0.03	0.26 ± 0.04	$F_{1,15}=0.85$ $p=0.58$	$F_{1,15}=12.15$ $p<0.01^{**}$	0.23 ± 0.03	0.25 ± 0.02	$F_{1,18}=0.57$ $p=0.56$	$F_{1,18}=1.79$ $p=0.31$	$F_{1,34}=4.51$ $p=0.04^{*}$
3-MT/DA	0.07 ± 0.01	0.06 ± 0.01	$F_{1,15}=0.65$ $p=0.59$	$F_{1,15}=9.87$ $p=0.01^{*}$	0.07 ± 0.01	0.06 ± 0.01	$F_{1,18}=1.05$ $p=0.50$	$F_{1,18}=2.04$ $p=0.31$	$F_{1,34}=1.72$ $p=0.20$

The values of each parameter are presented in means ± SDs in ng/ul of tissue and p-values for interactions were calculated by mixed model ANOVA with age, genotype and time as factors. The p-values for age and time were calculated by mixed model ANOVA grouped by genotype. p-values have been adjusted for multiple comparisons using the Benjamini-Hochberg-Yekutieli false discovery rate [FDR ($p <$ 0.05)].

*
p 0.05;

**
$p < 0.01$. NA, Noradrenaline; DOPAC, 3,4-Dihydroxyphenylacetic acid; DA, Dopamine; 5-HIAA, 5-Hydroxyindoleacetic acid; HVA, Homovanillic acid; 5-HT, Serotonin; 3-MT, 3-Methoxytyramine. WT, wild-type mice. MOR KO, mu opioid receptor knockout mice.

Table 4.

Wheel-running activity.

Time	WT (n=5)			MOR KO (n=5)				Period X Genotype	p for Period	p for Genotype
	Estimate	SE	95% CI	Estimate	SE	95% CI	Z			
Light phase	0	0	0	1.39	0.61	0.19 and 2.59	2.28	0.07	0.11	0.02 *
Dark phase	0	0	0	−0.23	0.24	−0.70 and 0.25	−0.94	0.83	0.09	0.35

The p-values for interactions were calculated by GENMOD with a negative binomial distribution with period and genotype as factors. The parameters and p-values for period and genotype were calculated by GENMOD with a negative binomial distribution with the interaction removed.

*
p 0.05;

**
p<0.01. WT, wild-type mice. MOR KO, mu opioid receptor knockout mice. SE, standard error. 95% CI, 95% confidence interval.

Author Manuscript Author Manuscript Author Manuscript Author Manuscript

Table 5.

Tail-flick test.

Groups	WT (1st, n=14; 2nd, n=5)			MOR KO (1st, n=14; 2nd, n=6)				Age X Genotype	Weight X Genotype	p for Age	p for Weight	p for Genotype
	Estimate	SE	95% CI	Estimate	SE	95% CI	Z					
1st cohort	0	0	0	−0.30	0.13	−0.55 and −0.05	−2.33	0.72	0.27	0.09	0.03 *	0.02 *
2nd cohort Midnight	0	0	0	−0.30	0.18	−0.65 and 0.05	−1.70	0.11	0.06	0.53	0.79	0.09
2nd cohort Midday	0	0	0	−0.42	0.11	−0.63 and −0.21	−3.95	0.19	0.23	0.75	0.25	<0.01 *
2nd cohort Ropinirole	0	0	0	0.17	0.10	−0.02 and 0.36	1.78	0.98	0.22	0.22	0.40	0.08

The p-values for interactions were calculated by GENMOD with a gamma distribution with age, weight, and genotype as factors. The parameters and p-values for age, weight and genotype were calculated by GENMOD with a gamma distribution with the interaction removed.

*
p 0.05;

**
p<0.01. WT, wild-type mice. MOR KO, mu opioid receptor knockout mice. SE, standard error. 95% CI, 95% confidence interval.